Precision calculation of the $\pi^- d$ scattering length and its impact on threshold πN scattering[☆]

V. Baru[a,b], C. Hanhart[a,c], M. Hoferichter[d], B. Kubis[d], A. Nogga[a,c], D. R. Phillips[d,e,*]

[a] *Institut für Kernphysik and Jülich Center for Hadron Physics, Forschungszentrum Jülich, D–52425 Jülich, Germany*
[b] *Institute for Theoretical and Experimental Physics, B. Cheremushinskaya 25, 117218 Moscow, Russia*
[c] *Institute for Advanced Simulation, Forschungszentrum Jülich, D–52425 Jülich, Germany*
[d] *Helmholtz-Institut für Strahlen- und Kernphysik and Bethe Center for Theoretical Physics, Universität Bonn, D–53115 Bonn, Germany*
[e] *Institute of Nuclear and Particle Physics and Department of Physics and Astronomy, Ohio University, Athens, OH 45701, USA*

Abstract

We present a calculation of the $\pi^- d$ scattering length with an accuracy of a few percent using chiral perturbation theory. For the first time isospin-violating corrections are included consistently. Using data on pionic deuterium and pionic hydrogen atoms, we extract the isoscalar and isovector pion–nucleon scattering lengths and obtain $a^+ = (7.6 \pm 3.1) \cdot 10^{-3} M_\pi^{-1}$ and $a^- = (86.1 \pm 0.9) \cdot 10^{-3} M_\pi^{-1}$. Via the Goldberger–Miyazawa–Oehme sum rule, this leads to a charged-pion–nucleon coupling constant $g_c^2/4\pi = 13.69 \pm 0.20$.

Keywords: Pion–baryon interactions, Chiral Lagrangians, Electromagnetic corrections to strong-interaction processes, Mesonic, hyperonic and antiprotonic atoms and molecules.

1. Introduction

Hadron–hadron scattering lengths are fundamental quantities characterizing the strong interaction, and are slowly becoming accessible to *ab initio* calculations in QCD [1, 2]. Among them, of particular interest are pion–hadron scattering lengths: the chiral symmetry of QCD and the Goldstone-boson nature of the pions dictate that they are small [3], and their non-vanishing size is linked to fundamental quantities like the light quark masses and condensates. Chiral symmetry in particular predicts that the isoscalar pion–nucleon scattering length a^+ is suppressed compared to its isovector counterpart a^-. A precise determination of a^+ would improve knowledge in many areas, e.g., dispersive analyses of the pion–nucleon σ-term [4], which measures the explicit chiral symmetry breaking in the nucleon mass due to up and down quark masses, and is, in turn, connected to the strangeness content of the nucleon. But, lack of π^0 beams and neutron targets makes direct pion–nucleon scattering experiments impossible in some charge channels, complicating a measurement of a^+; the only hope for future access to the $\pi^0 p$ scattering length lies in precision measurements of threshold neutral-pion photoproduction [5]. Thus, the combination of data and theory has, until now, lacked sufficient accuracy to even establish definitively that $a^+ \neq 0$. a^-, on the other hand, serves as a vital input to a determination of the pion–nucleon coupling constant via the Goldberger–Miyazawa–Oehme (GMO) sum rule [6]. While the uncertainty in a^- is much less than that in a^+, it still contributes significantly to the overall error bar on the sum-rule evaluation [7, 8]. This is one of several examples where data on pion–nucleon scattering affects more complicated systems like the nucleon–nucleon (NN) interaction, and hence has an impact on nuclear physics.

2. Pionic atoms

Within the last ten years new information on pion–nucleon scattering lengths has become available due to high-accuracy measurements of pionic hydrogen (πH). The most recent experimental results [9] are

$$\epsilon_{1s} = (-7.120 \pm 0.012)\,\text{eV}, \quad \Gamma_{1s} = (0.823 \pm 0.019)\,\text{eV}, \tag{1}$$

for the (attractive) shift of the $1s$ level of πH due to strong interactions and its width. These are connected,

[☆] Preprint no.: FZJ-IKP-TH-2010-05, HISKP-TH-10/06

[*] Corresponding author
Email address: phillips@phy.ohiou.edu (D. R. Phillips)

respectively, to the π^-–proton scattering length, a_{π^-p}, and the charge-exchange scattering length in the same channel [10]. ϵ_{1s} is related to a_{π^-p} through an improved Deser formula [11]

$$\epsilon_{1s} = -2\alpha^3\mu_H^2 a_{\pi^-p}(1 + K_\epsilon + \delta_\epsilon^{\rm vac}), \qquad (2)$$

where $\alpha = e^2/4\pi$, μ_H is the reduced mass of πH, $K_\epsilon = 2\alpha(1-\log\alpha)\mu_H a_{\pi^-p}$, and $\delta_\epsilon^{\rm vac} = 2\delta\Psi_H(0)/\Psi_H(0) = 0.48\%$ is the effect of vacuum polarization on the wave function at the origin [12]. Further, the width is given by [13]

$$\Gamma_{1s} = 4\alpha^3\mu_H^2 p_1\Big(1 + \frac{1}{P}\Big)(a_{\pi^-p}^{\rm cex})^2(1 + K_\Gamma + \delta_\epsilon^{\rm vac}), \qquad (3)$$

with

$$\begin{aligned} K_\Gamma &= 4\alpha(1 - \log\alpha)\mu_H a_{\pi^-p} \\ &\quad + 2\mu_H(m_{\rm p} + M_\pi - m_{\rm n} - M_{\pi^0})(a_{\pi^0 n})^2. \end{aligned} \qquad (4)$$

Here $m_{\rm p}$, $m_{\rm n}$, M_π, and M_{π^0} are the masses of the proton, the neutron, and the charged and neutral pions, respectively, p_1 is the momentum of the outgoing $n\pi^0$ pair, and the Panofsky ratio [14]

$$P = \frac{\sigma(\pi^- p \to \pi^0 n)}{\sigma(\pi^- p \to n\gamma)} = 1.546 \pm 0.009 \qquad (5)$$

incorporates the effect due to the radiative decay channel of πH. The pertinent scattering lengths are related to $a^\pm$ via [15]

$$a_{\pi^-p} = \tilde{a}^+ + a^- + \Delta\tilde{a}_{\pi^-p}, \;\; a_{\pi^-p}^{\rm cex} = -\sqrt{2}\,a^- + \Delta a_{\pi^-p}^{\rm cex}. \quad (6)$$

Throughout we follow the notation of Ref. [15] for the different πN channels, and have $\tilde{a}^+$ as a^+ plus a fixed shift explained below (see Sect. 3.4). The other shifts in Eq. (6) take values $\Delta\tilde{a}_{\pi^-p} = (-2.0 \pm 1.3)\cdot 10^{-3} M_\pi^{-1}$, and $\Delta a_{\pi^-p}^{\rm cex} = (0.4 \pm 0.9)\cdot 10^{-3} M_\pi^{-1}$ [15]. This accounts for isospin-violating effects up to next-to-leading order (NLO) in the chiral expansion.

Equations (2), (3), and (6) permit an extraction of a^- and $\tilde{a}^+$. However, further experimental information leads to better control of systematics and could enhance the accuracy of the scattering-length determination. Consequently, additional measurements of pion–nucleus atoms are of high interest—especially for atoms with isoscalar nuclei, as they provide better access to a^+. Here we use state-of-the-art theory to perform a combined analysis of the recent data for pionic deuterium (πD) as well as the numbers in Eq. (1) for πH. The resulting values for a^- and a^+ are of unprecedented accuracy.

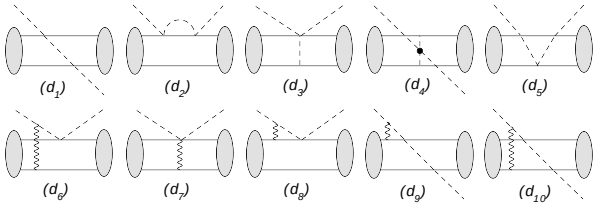

Figure 1: Topologies for $\pi^- d$ scattering. Solid, dashed, and wiggly lines denote nucleons, pions, and photons, respectively. The blobs indicate the deuteron wave functions.

In this work we focus on the strong shift, ϵ_{1s}^D, of the $1s$ level of pionic deuterium, which is related to the real part of the π^-–deuteron scattering length, $\mathrm{Re}\, a_{\pi^- d}$, by an improved Deser formula analogous to Eq. (2) [16]:

$$\epsilon_{1s}^D = -2\alpha^3\mu_D^2 \mathrm{Re}\, a_{\pi^- d}\left(1 + K_D + \delta_{\epsilon^D}^{\rm vac}\right). \qquad (7)$$

In Eq. (7) we have $\delta_{\epsilon^D}^{\rm vac} = 2\delta\Psi_D(0)/\Psi_D(0) = 0.51\%$ [12], $K_D = 2\alpha(1 - \log\alpha)\mu_D \mathrm{Re}\, a_{\pi^- d}$, and μ_D as the πD reduced mass.

3. The pion–deuteron scattering length

The real part of $a_{\pi^- d}$ can be decomposed into its two- and three-body contributions as:

$$\mathrm{Re}\, a_{\pi^- d} = a_{\pi^- d}^{(2)} + a_{\pi^- d}^{(3)}. \qquad (8)$$

It is in $a_{\pi^- d}^{(2)}$ that a^+ resides. Therefore, $a_{\pi^- d}^{(3)}$ must be calculated reliably if measurements of ϵ_{1s}^D are going to be profitably exploited to get information on a^+.

Thus, the bulk of the rest of this paper describes a calculation of $a_{\pi^- d}^{(3)}$ in chiral perturbation theory (χPT). This quantity can be expressed as

$$a_{\pi^- d}^{(3)} = a^{\rm str} + a^{\rm disp+\Delta} + a^{\rm EM}, \qquad (9)$$

where $a^{\rm str}$ defines the strong contribution, $a^{\rm disp+\Delta}$ involves two-nucleon and Δ-isobar–nucleon intermediate states, as well as diagrams with crossed pion lines, and $a^{\rm EM}$ involves photon-exchange contributions. This last piece is present because isospin violation from the up-down quark mass difference and electromagnetic effects must be taken into account (as in Ref. [15] we use a counting where $e \sim p$). Consistent consideration of such effects is a key advance made in this paper. We now deal with each of the contributions in Eq. (9), before returning to $a_{\pi^- d}^{(2)}$.

3.1. Strong contributions ($a^{\rm str}$)

The leading diagrams contributing to $a^{\rm str}$ are shown in the first line of Fig. 1. So far no counting scheme

is known that permits consistent, realistic, and simultaneous consideration of the two- and three-body operators which contribute to $\pi^- d$ scattering. However, each of these operators can be calculated independently, i.e. within its class, with a controlled uncertainty. In particular, Ref. [17] showed how the original counting by Weinberg [18, 19] can be modified such that the three-body contributions to $a_{\pi^- d}$ are calculated to very high accuracy. Since isospin breaking in the two-body sector is also well under control [15], this permits a precise extraction of $\tilde{a}^+$. Therefore, we now discuss the power counting for all contributions to $a^{\rm str}$ relative to the leading, $O(1)$, diagram (d_1).

In this counting there is a $(N^\dagger N)^2\pi^\dagger\pi$ contact term associated with the short-distance pieces of the integrals, which enters with an unknown coefficient at $O(p^2)$. This contribution cannot easily be determined from data, and is a key source of uncertainty in our result. With $p \sim M_\pi/m_{\rm p}$, we anticipate an accuracy of a few per cent for threshold $\pi^- d$ scattering. This expectation is substantiated by the sensitivity of our integrals to the choice of the deuteron wave function (see below). There we see a residual scale dependence of about 5%: an independent estimate of the contact term's effect.

But, to reach this accuracy, we must include all three-body terms up to $O(p^{3/2})$. In Ref. [20] it was shown that the sum of all NLO, $O(p)$, contributions vanishes in the isospin limit, corrections to which only enter at $O(p^3)$. Thus, the diagrams we need to consider up to $O(p)$ are (d_1)–(d_4) in Fig. 1. Note that although we count (d_5) as $O(p^2)$, its value is enhanced by a factor of π^2 due to its topology of two successive Coulombic propagators [17, 20]. Similar enhancements are present for all terms of the multiple-scattering series. Despite this, the multiple-scattering series converges quite quickly: we find from an explicit calculation that the sum of the first two terms (d_1) and (d_5) differs from the full result by only $0.1 \cdot 10^{-3} M_\pi^{-1}$. Note that the next diagram, where the pion leaves the two-nucleon system after four πN interactions on alternating nucleons, is logarithmically divergent, and therefore seems to necessitate a contact term. As the terms in the multiple-scattering series are enhanced as just described, we expect this contact term to also be enhanced. However, that enhancement is not enough to overcome the p^4 suppression relative to the leading, double-scattering, piece of $a_{\pi^- d}$, and so any such contact term has an appreciably smaller effect than the $O(p^2)$ contact term. Therefore its contribution does not impact the uncertainty estimate given above.

To achieve the requisite accuracy for our $\tilde{a}^+$ extraction we also need to include isospin-violating corrections from the different masses of the proton and neutron and charged and neutral pions in the diagrams (d_1)–(d_4). We then express the sum of diagrams in the first row of Fig. 1 as:

$$a^{\rm str} = a^{\rm static} + a^{\rm static}_{\rm NLO} + a^{\rm cut} + \Delta a^{(2)} + a^{\pi\pi} + a^{\rm triple}. \quad (10)$$

The first four terms arise from diagrams (d_1) and (d_2). However, (d_2) is partly accounted for in the two-body contribution $a^{(2)}_{\pi^- d}$. In order to treat the three-body dynamics properly we must replace the contribution of the two-body (πN) cut there by that of the three-body (πNN) cut [21]. The necessary integrals can be rearranged as in Eq. (10) (for details see [22]). $a^{\rm static}$ corresponds to (d_1) evaluated with a static pion propagator, and is numerically by far the dominant contribution. $a^{\rm static}_{\rm NLO}$ incorporates recoil corrections to the static pion propagator; $a^{\rm cut}$ comprises effects due to the three-body $\pi^0 nn$ and $\pi^- pn$ cuts, and $\Delta a^{(2)}$ emerges as an isospin-violating correction in this rearrangement. (In principle, there are also contributions with P-wave interactions between nucleons in the intermediate state, but they are of higher order.) Finally, $a^{\pi\pi}$ in Eq. (10) is determined by (d_3) and (d_4), while $a^{\rm triple}$ results from (d_5). Isospin-breaking corrections to the πN scattering lengths that appear in $a^{\rm str}$ are relevant only for $a^{\rm static}$, to which they contribute about 1%.

Our power counting is based on dimensional analysis assuming all integrals scale only with M_π. In fact, the integrals in Eq. (10) involve other scales too: $\sqrt{M_\pi \epsilon}$—due to the three-body cut—and $\sqrt{m_{\rm p}\epsilon}$, thanks to the deuterium wave functions (ϵ is the deuteron binding energy). At first glance, the presence of a three-body cut in the integral for $a^{\rm cut}$ makes it appear to be enhanced over its naive χPT order by $\sqrt{m_{\rm p}/M_\pi}$ [23]. However, this turns out not to be the case, because the Pauli principle and the spin-isospin character of the leading πN scattering operator ensure that the intermediate NN state in $(d_1) + (d_2)$ is projected onto a P-wave [21]. In consequence the scales $\sqrt{M_\pi \epsilon}$ and $\sqrt{m_{\rm p}\epsilon}$ do not enter the final result: any enhanced contribution cancels due to a subtle interplay between the two diagrams that is dictated by the Pauli principle. The combined integral is, as originally assumed in establishing the χPT ordering of diagrams, then dominated by momenta of order M_π.

The results for the pieces of $a^{\rm str}$ are given in Table 1. They produce a total:

$$a^{\rm str} = (-22.6 \pm 1.1 \pm 0.4) \cdot 10^{-3} M_\pi^{-1}. \quad (11)$$

The first error comes from the evaluation of all mentioned diagrams using different deuteron wave functions (we use NNLO chiral (five wave functions with different cutoffs) [24], CD Bonn [25], and AV 18 [26] poten-

Table 1: Strong contributions to $a^{(3)}_{\pi^- d}$ in units of $10^{-3} M_\pi^{-1}$. Here and below results are quoted for $a^- = 86.1 \cdot 10^{-3} M_\pi^{-1}$. For the band in Fig. 2 the full a^- dependence is taken into account.

$a^{\rm static}$	-24.1 ± 0.7	$a^{\rm static}_{\rm NLO}$	3.8 ± 0.2
$a^{\rm cut}$	-4.8 ± 0.5	$a^{\rm triple}$	2.6 ± 0.5
$a^{\pi\pi}$	-0.2 ± 0.3	$\Delta a^{(2)}$	0.2

tials), while the second is due to the uncertainty in the isospin-breaking shifts in the πN scattering lengths [15].

3.2. Photon loops ($a^{\rm EM}$)

Effects in this class due to photons with momenta of order αM_π are included in observables via the improved Deser formula. Thus, our calculation of $a^{(3)}_{\pi^- d}$ should include contributions from momenta above αM_π. The leading contributions due to the exchange of (Coulomb) photons of momenta of order M_π between the π^- and the proton are shown in the second row of Fig. 1: (d_6), (d_7), and (d_8). Photon exchange is perturbative at $|\mathbf{k}| \sim M_\pi$ (in contrast to the hadronic-atom regime where the photon ladder needs to be resummed), and the pertinent pieces of these graphs enter at $O(p)$ relative to (d_1). Such effects in the other diagrams are of a higher χPT order than we are considering here.

However, diagrams (d_6) and (d_8)–(d_{10}) are reducible in the sense originally defined by Weinberg [18], with the πNN intermediate state involving relative momenta of order $\sqrt{M_\pi \epsilon} \ll M_\pi$. Furthermore, in these diagrams, this state can occur with the NN pair in an S-wave, so we must also allow for the possibility of NN interactions while the pion is "in flight". When this is done we see that these four diagrams have an infrared divergence in the limit $\epsilon \to 0$, being enhanced by $\sqrt{M_\pi/\epsilon}$ as compared to their naive χPT order.

In order to avoid double counting we must also subtract from the resulting expressions for (d_6) and (d_8)–(d_{10}) (plus NN intermediate-state interactions) the quantum-mechanical interference between a zero-range (strong) pion–deuteron potential, proportional to $a_{\pi^- d}$, and the Coulomb interaction. That interference is already accounted for in the improved Deser formula (7). Note though, that Eq. (7) only accounts for intermediate-state pion (and deuteron) momenta of order αM_π. In particular, deuteron structure plays no role in its derivation.

After the pieces of (d_6) and (d_8)–(d_{10}) that are already included in Eq. (7) are removed the result is finite. The remaining, finite parts of (d_6) and (d_8)–(d_{10}) capture the effects of momenta $\gg \alpha M_\pi$ in these loops. These contributions are defined here to be part of $a_{\pi^- d}$, and must be calculated explicitly. In particular, they include effects in the loop which arise from the electromagnetic and pion–deuteron "form factors": the manner in which the finite extent of the deuteron modifies the loop integral for momenta well above the hadronic atom scale αM_π [22].

This contribution to $a_{\pi^- d}$ is ostensibly large, since it is an infrared-sensitive integral that potentially has contributions from momenta of order $\sqrt{M_\pi \epsilon}$. But, analysis analogous to Ref. [27] shows that this particular piece of the integral is zero because of symmetry arguments. When the NN pair is in an S-wave it can be written as a sum of overlaps between NN wave functions in the continuum and the deuteron bound state, and orthogonality then guarantees that the result is zero. In the case of an intermediate NN P-wave pair it is the Pauli principle that causes the cancellation [22].

There is still a possible contribution in the loop from momenta of order $\sqrt{m_{\rm p} \epsilon}$. This would be enhanced by $M_\pi/\sqrt{m_{\rm p}\epsilon}$ compared to its naive χPT order, and so could be relevant for our analysis. Direct evaluation of this part of (d_6) and (d_8)—including the diagrams with NN interactions in an S-wave—yields a contribution to $a_{\pi^- d}$ of $-0.04\,\tilde{a}^+$. (Isospin-breaking shifts of $\tilde{a}^+$ can be added here, but do not change the prefactor.) Replacing the single πN scattering of these diagrams by double scattering as in (d_9) and (d_{10}) gives effects larger by a factor of $a_{\pi^- d}/2\tilde{a}^+$, but, despite their being infrared enhanced, the impact of such pieces on $a_{\pi^- d}$ is still significantly less than our theoretical uncertainty.

This leaves us needing to consider only effects from momenta M_π in diagrams (d_6)–(d_8). As with (d_2) in $a^{\rm str}$, parts of these diagrams are already included in $a^{(2)}_{\pi^- d}$, but this can be dealt with along the same lines [22]. The result is:

$$a^{\rm EM} = (0.94 \pm 0.01) \cdot 10^{-3} M_\pi^{-1}, \qquad (12)$$

where the error again reflects the wave-function dependence. Thus, virtual photons with $|\mathbf{k}| \sim M_\pi$ increase Re $a_{\pi^- d}$ by about 4%.

3.3. Dispersive and Delta(1232) corrections ($a^{\rm disp+\Delta}$)

These produce effects in $a_{\pi^- d}$ that scale with half-integer powers of p [28, 29]. Their leading contribution is $O(p^{3/2})$ relative to (d_1), and is computed here using a calculation for $NN \to d\pi$ up to NLO in χPT [30]. Note that although we include Delta(1232) effects in the $\pi NN \to \pi NN$ transition operator, it is not necessary to account for the Delta(1232) as an explicit degree of freedom when computing the deuteron wave function. Its effects in the NN potential at energies of order ϵ enter

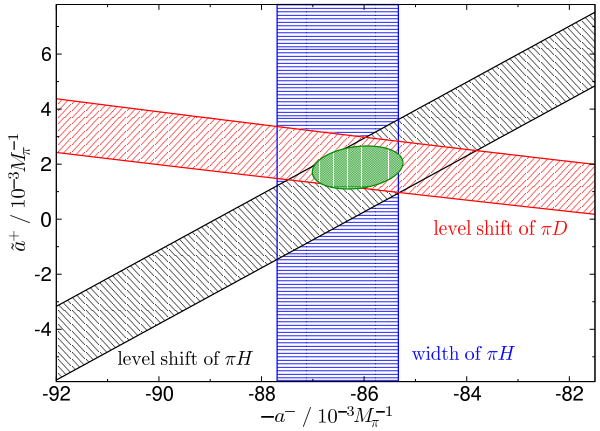

Figure 2: Combined constraints in the $\tilde{a}^+$–a^- plane from data on the width and energy shift of πH, as well as the πD energy shift.

only at relative $O(p^2)$ [29]. In Refs. [28, 29] all integrals were cut off at 1 GeV; we have checked that this does not introduce additional uncertainty and obtain:

$$a^{\text{disp+}\Delta} = (-0.6 \pm 1.5) \cdot 10^{-3} M_\pi^{-1}. \tag{13}$$

Since this is at the limit of our desired accuracy we need not include isospin-violating corrections to $a^{\text{disp+}\Delta}$.

3.4. The two-body part ($a^{(2)}_{\pi^- d}$)

As alluded to above, it is not possible to isolate a^+ in analyses of πH and πD. Information on the isoscalar scattering length can only be extracted as a combination $\tilde{a}^+$, in which the low-energy constants c_1 (which occurs because its impact on a^+ is proportional to the neutral-pion mass squared) and f_1 (which denotes the leading isoscalar electromagnetic correction) also appear [16]:

$$\tilde{a}^+ \equiv a^+ + \frac{1}{1 + M_\pi/m_\text{p}} \left\{ \frac{M_\pi^2 - M_{\pi^0}^2}{\pi F_\pi^2} c_1 - 2\alpha f_1 \right\}. \tag{14}$$

In the two-body part of $a_{\pi^- d}$, $\tilde{a}^+$ is further shifted, as shown in the NLO analysis of Ref. [15]:

$$\begin{aligned} a^{(2)}_{\pi^- d} &= \frac{2\mu_D}{\mu_H} \left(\tilde{a}^+ + \Delta\tilde{a}^+\right), \\ \Delta\tilde{a}^+ &= (-3.3 \pm 0.3) \cdot 10^{-3} M_\pi^{-1}. \end{aligned} \tag{15}$$

4. Results and Discussion

We now add together all the individual contributions. Amusingly, most of the additional three-body corrections considered in this study accidentally cancel: $\Delta a^{(2)} + a^{\text{static}}_{\text{NLO}} + a^{\text{cut}} + a^{\text{EM}} = (0.1 \pm 0.7) \cdot 10^{-3} M_\pi^{-1}$. For this reason, the main impact of our analysis on the extraction of pion–nucleon scattering lengths turns out to be due to the NLO isospin-breaking corrections in the two-body part [31].

Table 2: Individual contributions to the error on $\tilde{a}^+$ are added in quadrature to obtain the uncertainty depicted in the bands of Fig. 2. Each row below gives the impact of one source of error as a percentage of that total. The first row is the impact of the experimental uncertainty in ϵ^D_{1s}, the second gives the uncertainty in the isospin-breaking shifts of πN scattering lengths that occur in a^{str}, and the third row is the uncertainty in $\Delta\tilde{a}^+$ according to Eq. (15). The final two rows show the impact of uncertainties in our calculation of $\text{Re}\, a^{(3)}_{\pi^- d}$, as described in the text.

ϵ^D_{1s}	16%
$\Delta\tilde{a}_{\pi^- p}, \Delta a^{\text{cex}}_{\pi^- p}$	21 %
$\Delta\tilde{a}^+$	30 %
$a^{\text{disp+}\Delta}$	75%
Wave-function averages	53%

The energy shift of πD has recently been remeasured as [32]

$$\epsilon^D_{1s} = (2.356 \pm 0.031)\,\text{eV}. \tag{16}$$

Combining this result, the dependence of the $\pi^- d$ scattering length on $\tilde{a}^+$ and a^-, and the results for πH discussed above, we find the constraints depicted in Fig. 2. The combined 1σ error ellipse yields

$$\tilde{a}^+ = (1.9 \pm 0.8) \cdot 10^{-3} M_\pi^{-1}, \;\; a^- = (86.1 \pm 0.9) \cdot 10^{-3} M_\pi^{-1}, \tag{17}$$

with a correlation coefficient $\rho_{a^- \tilde{a}^+} = -0.21$. We find that the inclusion of the πD energy shift reduces the uncertainty of $\tilde{a}^+$ by more than a factor of 2. Note that in the case of the πH level shift the width of the band is dominated by the theoretical uncertainty in $\Delta\tilde{a}_{\pi^- p}$, whereas for the πH width the experimental error is about 50% larger than the theoretical one. The uncertainty in $a^{\text{disp+}\Delta}$ is the largest contribution to the πD error band, see Table 2. The wave-function averages contribute about $0.5 \cdot 10^{-3} M_\pi^{-1}$ to the overall uncertainty in $\tilde{a}^+$, which is in line with the estimated impact on $a_{\pi^- d}$ of the $O(p^2)$—relative to (d_1)—contact term.

Taken together with $c_1 = (-1.0 \pm 0.3)\,\text{GeV}^{-1}$ [22] and the rough estimate $|f_1| \leq 1.4\,\text{GeV}^{-1}$ [33], Eq. (17) yields a non-zero a^+ at better than the 95% confidence level:

$$a^+ = (7.6 \pm 3.1) \cdot 10^{-3} M_\pi^{-1}. \tag{18}$$

The final result for a^+ is only a little larger than several of the contributions considered in our analysis. This emphasizes the importance of a systematic ordering scheme, and a careful treatment of isospin violation

and three-body dynamics. A reduction of the theoretical uncertainty beyond that of the present analysis will be hard to achieve without additional QCD input that helps pin down the unknown contact-term contributions in both the πN and πNN sectors.

Finally, these results allow us to infer the charged-pion–nucleon coupling constant, g_c, from the GMO sum rule, with isospin-violating corrections to the πN scattering lengths fully under control for the first time. Inspired by Ref. [7], we take $a_{\pi^- p}$ extracted from Eq. (2), $a_{\pi^- p} + a_{\pi^- n}$ from our $a_{\pi^- d}$ analysis, and $a_{\pi^- n} - a_{\pi^+ p}$ from Ref. [15], yielding $g_c^2/4\pi = 13.69 \pm 0.12 \pm 0.15$ [22]. (Here the first error is due to the scattering lengths and the second to an integral over $\pi^\pm p$ cross sections [7, 8].) This is in agreement with determinations from NN [34] and πN [35] scattering data.

Acknowledgments

We thank D. Gotta, A. Kudryavtsev, U.-G. Meißner, A. Rusetsky, M. Sainio, and A. W. Thomas for useful discussions. This research was supported by the DFG (SFB/TR 16, "Subnuclear Structure of Matter"), DFG-RFBR grant (436 RUS 113/991/0-1), the Mercator Programme of the DFG, the Helmholtz Association through funds provided to the virtual institute "Spin and strong QCD" (VH-VI-231) and the young investigator group "Few-Nucleon Systems in Chiral Effective Field Theory" (grant VH-NG-222), the Bonn-Cologne Graduate School of Physics and Astronomy, the project "Study of Strongly Interacting Matter" (HadronPhysics2, grant No. 227431) under the 7th Framework Programme of the EU, the US Department of Energy (Office of Nuclear Physics, under contract No. DE-FG02-93ER40756 with Ohio University), and the Federal Agency of Atomic Research of the Russian Federation ("Rosatom"). Computing resources were provided by the JSC, Jülich, Germany.

References

[1] S. R. Beane, K. Orginos and M. J. Savage, Int. J. Mod. Phys. E **17** (2008) 1157 [arXiv:0805.4629 [hep-lat]].
[2] A. Torok *et al.*, Phys. Rev. D **81** (2010) 074506 [arXiv:0907.1913 [hep-lat]].
[3] S. Weinberg, Phys. Rev. Lett. **17** (1966) 616.
[4] J. Gasser, H. Leutwyler, and M. E. Sainio, Phys. Lett. B **253** (1991) 252.
[5] A. M. Bernstein, M. W. Ahmed, S. Stave, Y. K. Wu and H. R. Weller, Ann. Rev. Nucl. Part. Sci. **59** (2009) 115 [arXiv:0902.3650 [nucl-ex]]; A. M. Bernstein, Phys. Lett. B **442** (1998) 20 [arXiv:hep-ph/9810376].
[6] M. L. Goldberger, H. Miyazawa and R. Oehme, Phys. Rev. **99** (1955) 986.
[7] T. E. O. Ericson, B. Loiseau and A. W. Thomas, Phys. Rev. C **66** (2002) 014005 [arXiv:hep-ph/0009312].
[8] V. V. Abaev, P. Metsä and M. E. Sainio, Eur. Phys. J. A **32** (2007) 321 [arXiv:0704.3167 [hep-ph]].
[9] D. Gotta *et al.*, Lect. Notes Phys. **745** (2008) 165.
[10] J. Gasser, V. E. Lyubovitskij, and A. Rusetsky, Phys. Rept. **456** (2008) 167 [arXiv:0711.3522 [hep-ph]].
[11] V. E. Lyubovitskij and A. Rusetsky, Phys. Lett. B **494** (2000) 9 [arXiv:hep-ph/0009206].
[12] D. Eiras and J. Soto, Phys. Lett. B **491** (2000) 101 [arXiv:hep-ph/0005066].
[13] P. Zemp, PhD thesis, University of Bern (2004).
[14] J. Spuller *et al.*, Phys. Lett. B **67** (1977) 479.
[15] M. Hoferichter, B. Kubis, and U.-G. Meißner, Phys. Lett. B **678** (2009) 65 [arXiv:0903.3890 [hep-ph]]; Nucl. Phys. A **833** (2010) 18 [arXiv:0909.4390 [hep-ph]].
[16] U.-G. Meißner, U. Raha, and A. Rusetsky, Phys. Lett. B **639** (2006) 478 [arXiv:nucl-th/0512035]; Eur. Phys. J. C **41** (2005) 213 [arXiv:nucl-th/0501073].
[17] S. Liebig, V. Baru, F. Ballout, C. Hanhart, and A. Nogga, arXiv:1003.3826 [nucl-th].
[18] S. Weinberg, Phys. Lett. B **295** (1992) 114 [arXiv:hep-ph/9209257].
[19] S. R. Beane, V. Bernard, T. S. H. Lee and U.-G. Meißner, Phys. Rev. C **57** (1998) 424 [arXiv:nucl-th/9708035].
[20] S. R. Beane, V. Bernard, E. Epelbaum, U.-G. Meißner, and D. R. Phillips, Nucl. Phys. A **720** (2003) 399 [arXiv:hep-ph/0206219].
[21] V. Baru, C. Hanhart, A. E. Kudryavtsev, and U.-G. Meißner, Phys. Lett. B **589** (2004) 118 [arXiv:nucl-th/0402027].
[22] V. Baru, C. Hanhart, M. Hoferichter, B. Kubis, A. Nogga, D. R. Phillips, in preparation.
[23] V. Lensky, V. Baru, J. Haidenbauer, C. Hanhart, A. E. Kudryavtsev, and U.-G. Meißner, Eur. Phys. J. A **26** (2005) 107 [arXiv:nucl-th/0505039].
[24] E. Epelbaum, W. Glöckle, and U.-G. Meißner, Nucl. Phys. A **747** (2005) 362 [arXiv:nucl-th/0405048].
[25] R. Machleidt, Phys. Rev. C **63** (2001) 024001 [arXiv:nucl-th/0006014].
[26] R. B. Wiringa, V. G. J. Stoks, and R. Schiavilla, Phys. Rev. C **51** (1995) 38 [arXiv:nucl-th/9408016].
[27] V. Baru, E. Epelbaum, and A. Rusetsky, Eur. Phys. J. A **42** (2009) 111 [arXiv:0905.4249 [nucl-th]].
[28] V. Lensky, V. Baru, J. Haidenbauer, C. Hanhart, A. E. Kudryavtsev, and U.-G. Meißner, Phys. Lett. B **648** (2007) 46 [arXiv:nucl-th/0608042].
[29] V. Baru, J. Haidenbauer, C. Hanhart, A. E. Kudryavtsev, V. Lensky, and U.-G. Meißner, Phys. Lett. B **659** (2008) 184 [arXiv:0706.4023 [nucl-th]].
[30] V. Lensky, V. Baru, J. Haidenbauer, C. Hanhart, A. E. Kudryavtsev, and U.-G. Meißner, Eur. Phys. J. A **27** (2006) 37 [arXiv:nucl-th/0511054].
[31] M. Hoferichter, B. Kubis, and U.-G. Meißner, PoS **CD09** (2009) 014 [arXiv:0910.0736 [hep-ph]].
[32] D. Gotta, private communication; Th. Strauch *et al.*, EPJ Web Conf. **3** (2010) 03006 [arXiv:1002.4277 [nucl-ex]].
[33] J. Gasser, M. A. Ivanov, E. Lipartia, M. Mojžiš, and A. Rusetsky, Eur. Phys. J. C **26** (2002) 13 [arXiv:hep-ph/0206068]; N. Fettes and U.-G. Meißner, Phys. Rev. C **63** (2001) 045201 [arXiv:hep-ph/0008181].
[34] J. J. de Swart, M. C. M. Rentmeester and R. G. E. Timmermans, PiN Newslett. **13** (1997) 96 [arXiv:nucl-th/9802084].
[35] R. A. Arndt, R. L. Workman and M. M. Pavan, Phys. Rev. C **49** (1994) 2729.